Applied Physics Letters

RESEARCH ARTICLE | DECEMBER 30 2025

Spontaneous generation of athermal phonon bursts within bulk silicon causing excess noise, low energy background events, and quasiparticle poisoning in superconducting sensors

C. L. Chang ; Y.-Y. Chang ; M. Garcia-Sciveres ; W. Guo ; S. A. Hertel ; X. Li ; J. Lin ; M. Lisovenko ; R. Mahapatra ; W. Matava ; D. N. McKinsey; P. K. Patel ; B. Penning ; H. D. Pinckney ; M. Platt; M. Pyle ; Y. Qi ; M. Reed ; I. Rydstrom ; R. K. Romani ; B. Sadoulet ; B. Serfass ; P. Sorensen ; B. Suerfu ; V. Velan ; G. Wang ; Y. Wang ; M. R. Williams ; V. G. Yefremenko; TESSERACT Collaboration

Appl. Phys. Lett. 127, 263502 (2025)
https://doi.org/10.1063/5.0281876
CHORUS

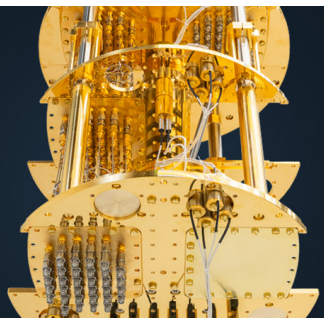

Applied Physics Letters ARTICLE pubs.aip.org/aip/apl

Spontaneous generation of athermal phonon bursts within bulk silicon causing excess noise, low energy background events, and quasiparticle poisoning in superconducting sensors

Cite as: Appl. Phys. Lett. **127**, 263502 (2025); doi: 10.1063/5.0281876
Submitted: 22 May 2025 · Accepted: 29 October 2025 ·
Published Online: 30 December 2025

View Online Export Citation CrossMark

C. L. Chang,[1,2,3] Y.-Y. Chang,[4] M. Garcia-Sciveres,[5,6] W. Guo,[7,8] S. A. Hertel,[9] X. Li,[5] J. Lin,[4,5] M. Lisovenko,[1] R. Mahapatra,[10] W. Matava,[4] D. N. McKinsey,[4,5] P. K. Patel,[9] B. Penning,[11] H. D. Pinckney,[9] M. Platt,[10] M. Pyle,[4] Y. Qi,[7,8] M. Reed,[4] I. Rydstrom,[4] R. K. Romani,[4,a)] B. Sadoulet,[4] B. Serfass,[4] P. Sorensen,[5] B. Suerfu,[6] V. Velan,[5] G. Wang,[1] Y. Wang,[4,5] M. R. Williams,[5] V. G. Yefremenko,[1] and TESSERACT Collaboration

AFFILIATIONS

[1]Argonne National Laboratory, 9700 S Cass Ave, Lemont, Illinois 60439, USA
[2]Kavli Institute for Cosmological Physics, The University of Chicago, 5640 S Ellis Ave., Chicago, Illinois 60637, USA
[3]Department of Astronomy and Astrophysics, The University of Chicago, Eckhardt, 5640 S Ellis Ave., Chicago, Illinois 60637, USA
[4]Department of Physics, University of California Berkeley, 366 LeConte Hall 7300, Berkeley, California 94720, USA
[5]Lawrence Berkeley National Laboratory, 1 Cyclotron Rd., Berkeley, California 94720, USA
[6]International Center for Quantum-Field Measurement Systems for Studies of the Universe and Particles (QUP, WPI), High Energy Accelerator Research Organization (KEK), Oho 1-1, Tsukuba, Ibaraki 305-0801, Japan
[7]Department of Mechanical Engineering, FAMU-FSU College of Engineering, Florida State University, 2525 Pottsdamer Street, Tallahassee, Florida 32310, USA
[8]National High Magnetic Field Laboratory, 1800 E Paul Dirac Dr., Tallahassee, Florida 32310, USA
[9]University of Massachusetts, Amherst Center for Fundamental Interactions and Department of Physics, 101 Stockbridge Hall, 80 Campus Center Way, Amherst, Massachusetts 01003-9337, USA
[10]Department of Physics and Astronomy, Texas A&M University, 4242 TAMU, 578 University Dr., College Station, Texas 77843-4242, USA
[11]Department of Physics, University of Zurich, Winterthurerstrasse 190, 8057 Zurich, Switzerland

[a)]**Author to whom correspondence should be addressed:** rkromani@berkeley.edu

ABSTRACT

Solid state phonon detectors used in the search for dark matter and coherent neutrino nucleus interactions (CE ν NS) require excellent energy resolution (eV-scale or below) and low backgrounds. An unknown source of phonon bursts, the low energy excess (LEE), dominates other above-threshold backgrounds and generates excess shot noise from subthreshold bursts. In this paper, we measure these phonon bursts for 12 days after cooldown in two nearly identical 1 cm^2 silicon detectors that differ only in the thickness of their substrate (1 vs 4 mm thick). We find that both the channel-correlated shot noise and near-threshold shared LEE relax with time since cooldown. Additionally, both the correlated shot noise and LEE rates scale linearly with substrate thickness. When combined with previous measurements of other silicon phonon detectors with different substrate geometries and mechanical support strategies, these measurements strongly suggest that the dominant source of both above and below threshold LEE is the bulk substrate. By monitoring the relation between bias power and excess phonon shot noise, we estimate that the energy scale for subthreshold noise events is 0.68 ± 0.38 meV. In our final dataset, we report a world-leading energy resolution of 258.5 ± 0.4 meV in the 1 mm thick detector. Simple calculations suggest that these silicon substrate phonon bursts are likely a significant source of quasiparticle poisoning in superconducting qubits operated in well shielded and vibration free environments.

Solid state phonon detectors with excellent energy resolution and low backgrounds are a key technology with applications in fundamental physics and beyond. For example, the search for light dark matter candidates[1–5] and the detection of rare eV-scale Coherent Elastic Neutrino Nucleus Scattering (CE ν NS) from nuclear reactors[6,7] require detectors with both low noise and low background rates to probe new regions of parameter space. High-resolution phonon sensors can also be used as a veto[8] in photon-coupled rare event searches (e.g., dark photon or axion searches[9,10]).

Unfortunately, today's low-threshold phonon detectors observe orders of magnitude more background events below several hundred eV than expected from background radioactivity or cosmic ray interactions.[11,12] These events are often referred to as the "low energy excess" (LEE). Measurements[13,14] show that the LEE can be categorized into two distinct subclasses based on the channel energy partition in detectors with multichannel phonon sensor readout. "Single" LEE events are found to deposit nearly all of their energy in a single phonon sensor channel, suggesting that they originate within the metal films of the phonon sensors themselves. By contrast, "shared" LEE events deposit nearly equal amounts of energy in all phonon sensor channels, which suggests a substrate origin. Similarly, our collaboration has observed both channel-correlated and uncorrelated excess noise in our phonon sensors, consistent with shot noise from subthreshold events from these two classes.[14] This work probes the scaling of these backgrounds and noise terms with substrate thickness to further understand their origin.

Here, we measure background events and noise in two nominally identical 1 cm^2 silicon low-threshold athermal phonon detectors, where the silicon substrate thickness was varied from 1 mm (mass: 0.233 g) to 4 mm (mass: 0.932 g) (Fig. 1). To readout phonon signals, the detectors use W Transition Edge Sensors (TES, $T_c \approx 50$ mK) coupled to aluminum phonon collection fins in the common Quasiparticle-trap-enhanced Electrothermal-feedback Transition Edge Sensor (QET)[15] architecture, employing an identical design to the detectors in Ref. 14. These individual phonon sensors are aggregated into two separately readout channels to distinguish events and noise, which deposit energy in a single phonon sensor from those that deposit energy in multiple phonon sensors.[13,14,16] The phonon sensors on these detectors have improved phonon energy collection efficiency, saturation energy, and channel uniformity compared to those from an earlier fabrication run that suffered from accidental W over-etching.[14] As in Ref. 17, both detectors are suspended by wire bonds to suppress backgrounds associated with detector holding and housed together in an IR and EMI shielded set of housings attached to the mixing chamber stage of a dilution refrigerator. They were readout using single-stage DC SQUID array amplifiers.

To minimize LEE rate differences due to uncontrolled systematic variables, differences in fabrication, transport, storage, and measurement were minimized to the extent possible. Both detector substrates were detector-grade double side polished intrinsic silicon (70 k Ω cm for 1 mm thick and 20 k Ω cm for 4 mm thick). The detectors were fabricated in the same facility at Texas A&M using identical procedures in consecutive fabrication runs separated by less than one week. Since LEE is known to potentially vary with time and thermal cycling, the detectors were transported, diced, stored, and run together in the same experimental setup at UC Berkeley using nominally identical electronic channels. Unfortunately, the detectors displayed different susceptibility

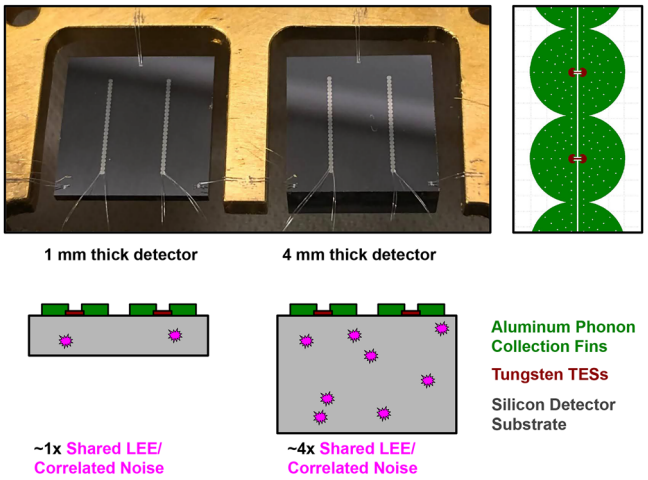

FIG. 1. (Top left) Photograph of our 1 mm (left) and 4 mm thick (right) 1 cm^2 silicon detectors. (Top right) Detail on mask design for our phonon sensors (QETs). For scale, the QET fins have a radius of approximately 140 μm. (Bottom) Sketch of backgrounds and shot noise sources we observe in our devices. Shared LEE backgrounds and correlated phonon shot noise appear at approximately 4x the rate in the 4 mm detector compared to the 1 mm detector.

to environmental vibrations, which we believe is due to uncontrolled variability in the wirebond hanging process.

To calibrate our detectors' response, we illuminate the phonon sensor face with pulses of 450 nm (2.755 eV) photons, emitted from a diffuser at the tip of a single mode fiber, which runs from the detector cavity to a room temperature laser. To precisely record the time of photon calibration events, a logic level signal from the signal generator that powers the laser is concurrently recorded and stored with the continuously recorded signal data streams. Phonon signal amplitudes are then estimated offline using optimum filters.[14,18] Plotting the height of the resulting events in each channel (Fig. 2, left), we observe the same features as in Ref. 14. Most photons are absorbed in the detector substrate system and produce approximately equal responses in both channels, while occasionally photons are directly absorbed by the aluminum phonon collection fins, producing a large saturated response in only one channel. Because multiple photons may strike the detector in one laser pulse, we also observe a superposition of these event types.

To combine the responses of the two channels of one detector, we use a "2 × 1" multichannel optimum filter, which simultaneously fits the response in both channels, scaling them together by one amplitude.[14,18] In our final dataset, we achieve a baseline phonon energy resolution of 258.5 ± 0.4 meV for this combined channel response, improving upon the resolution of our previously world-leading detector[14,18] and prior work by other groups.[19,20]

We periodically calibrate our detector and find that the energy resolution of both detectors monotonically improves over the course of the run (Fig. 2, Bottom Right). In principle, this could be due to two factors: an improvement in the sensors' phonon collection efficiency over time or a reduction in noise in the detector. Monitoring our detectors' phonon collection efficiencies over time, we find that they are approximately constant (see the supplementary material Sec. A), implying that our noise environment is improving with time.

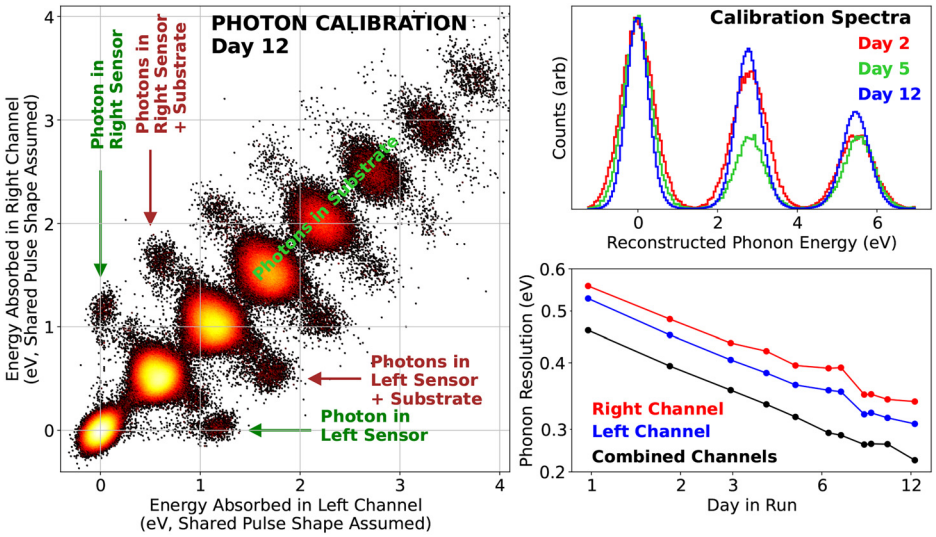

FIG. 2. 1 mm device calibration. (Left) Two dimensional histogram of calibration events. Most calibration photons hit the substrate, causing even responses in both channels (main diagonal events). Due to the energy resolution of our detector, individual photons appear as quantized quasi-Gaussian groups. Occasionally, photons hit a phonon sensor (QET), causing a large response in that channel (offset events). Around 1.1 eV of each 2.755 eV, photon is absorbed in our sensors due to our phonon collection efficiency. (Top right) Photon calibration spectra taken on days 2, 5, and 12. Note the improvement on baseline resolution over time. (Bottom right) Measured phonon energy resolutions in the right, left, and combined channels over time.

To characterize our detectors' noise over time, we record 2 h of continuous data following each calibration dataset and remove time periods with abnormally low bias power, which is primarily caused by unusually high environmental vibrations or large energy depositions. Additionally, to select periods without above-threshold events that would contaminate and bias our noise, we find the largest magnitude pulse in the entire 200 ms period using an optimal filter and select periods for which this fit has a negative amplitude, i.e., the largest event in the trace is a statistical fluctuation rather than a real energy deposition. In total, 3.9% of the 200 ms traces pass these very strict noise selection criteria and are used to estimate the noise Cross Power Spectral Density (CSD, see the supplementary material Sec. C for further discussion of our cuts). We reference this CSD to noise equivalent power by applying a three-pole responsivity model[21,22] for each channel [i.e., $\partial P/\partial I(f)$] that is estimated from IV and $\frac{\partial I}{\partial V}$ measurements as in Ref. 14.

Similar to our observations in Ref. 14, we find that the noise is significantly larger than the expected theoretical TES noise[22] and has a significant broad band channel-correlated component (which should be statistically consistent with zero). The broad spectrum correlated noise is consistent with shot noise from many subthreshold phonon events in the substrate; i.e., it has the same frequency shape and channel energy partition ($\sim$50% left, $\sim$50% right) as substrate-interacting calibration photons (Fig. 3, Top Right). The magnitude of this broad correlated noise appears to scale with the detector volume, since the correlated noise is four times larger in the 4 mm detector than in the 1 mm detector (Fig. 3, Top Right).

After removing these correlated noise terms, we find that there is an additional quasi-flat uncorrelated noise term, in significant excess of the expected level of thermal fluctuation noise in the TESs, but in some tension with the flat shot noise model of Ref. 14 (see the supplementary material Sec. D for further discussion).

Repeating this measurement of the correlated phonon noise amplitude, we are able to plot the correlated noise measured in the detector as a function of time (see Fig. 4). As with the phonon energy resolution, we find that the correlated phonon noise drops with time, causing the resolution improvement with time.

We additionally find that the TES bias power (i.e., the power applied to the TES to keep it in transition) increases substantially over time (see Fig. 4). We assume that this increase over time is essentially entirely due to a decreasing parasitic power over time, as shifts in bias power due to a cooling dilution fridge base (mixing chamber, MC) temperature should be very small (see the supplementary material Sec. B). As with the correlated noise, the shift in the bias power over time is approximately four times larger in the 4 mm detector than in the 1 mm detector.

As shown in Fig. 4, right, the correlated noise and bias power are found to be linearly related for all times in both detectors, thus share an identical functional dependence on time. This strongly suggests that both observations are caused by the same underlying mechanism.

To gain insight with a simple benchmark model, a random process in which a quantized energy deposition ε occurs with an average rate $R(t)$ that scales with the detector thickness, and $t^{-\kappa}$ will produce a parasitic power and excess shot noise of

$$P_{1,par} = \varepsilon R(t) = \varepsilon R_0 t^{-\kappa}, \quad (1)$$

$$P_{4,par} = \varepsilon 4R(t) = \varepsilon 4R_0 t^{-\kappa}, \quad (2)$$

$$S_{1,ex} = 2\varepsilon^2 R(t) = 2\varepsilon^2 R_0 t^{-\kappa} = 2\varepsilon P_{1,par}, \quad (3)$$

$$S_{4,ex} = 8\varepsilon^2 R(t) = 8\varepsilon^2 R_0 t^{-\kappa} = 2\varepsilon P_{4,par}. \quad (4)$$

We plot the excess correlated noise and bias power as a function of time and find good agreement with this model (an exponential trend is not a good fit to the data). We find $\varepsilon = 0.68 \pm 0.38$ meV and $\kappa = 0.635 \pm 0.009$. While the characteristic energy scale ε seems to remain constant over time, there is no reason to assume that the shot noise events all have an identical energy. As discussed in supplementary material Sec. E, ϵ is readily generalizable to processes, which have a distribution of energy depositions, where $\varepsilon = \frac{\langle E^2 \rangle}{\langle E \rangle}$. So long as the distribution is not e.g., double peaked, ε can still be thought of as a characteristic energy scale of the underlying phonon burst process.

For steep exponential and power law spectra, ε is on the order of the low energy cutoff to the spectrum. This offers a potential explanation for why the measured ε is comparable to the aluminum

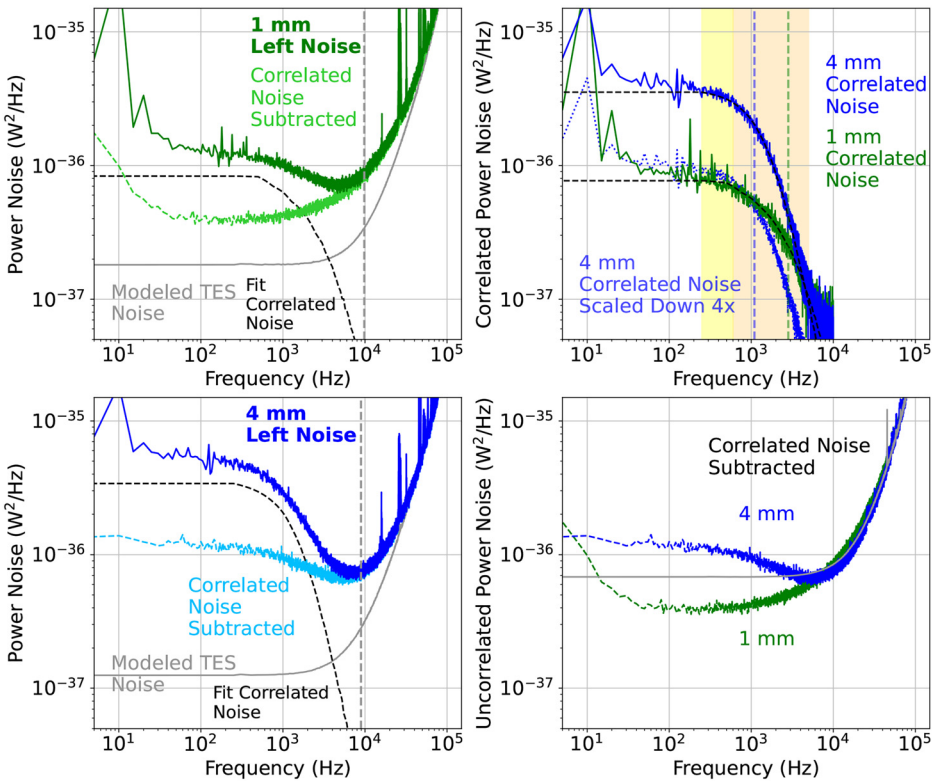

FIG. 3. (Left) Noise in the left channels of the 1 mm (top, green) and 4 mm (bottom, blue) detectors. Our noise is well in excess of our modeled TES noise (gray, dotted) and is composed of correlated phonon noise and uncorrelated noise as in Ref. 14. The peaks around 150 Hz are due to vibration coupled noise. Gray dashed lines show the primary (electrothermal) pole of the TES. (Top right) Correlated noise (i.e., off diagonal CSD element S_{LR}) in the 4 and 1 mm detectors. The correlated noise in the 4 mm detector is four times as large as the 1 mm detector. The amplitude of the 1 mm correlated noise is fit in the orange highlighted region (to avoid vibration coupled peaks), while the 4 mm noise is fit in the orange and yellow regions. Dashed green and blue lines show the primary phonon poles of the 1 and 4 mm detectors, respectively. (Bottom right) Uncorrelated noise (i.e., S_{LL}, with the modeled correlated noise subtracted) in the left channels of the 1 and 4 mm detectors, consistent with the modeled TES Johnson noise at high frequencies and an excess noise term that is approximately flat and consistent between the two channels at low frequencies (see supplementary material Sec. F for further discussion). Data correspond to the final (day 12) dataset.

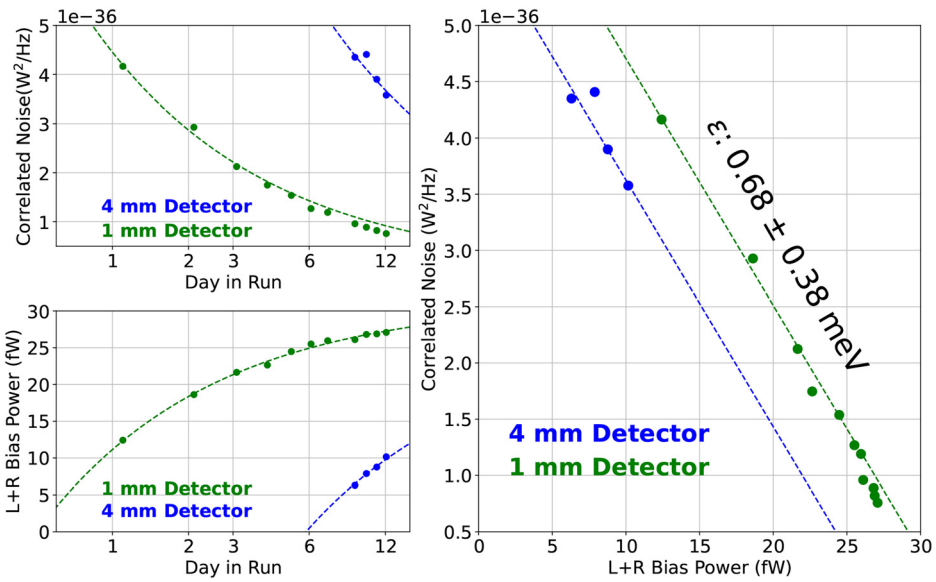

FIG. 4. Correlated noise level (top left) and Left + Right channel bias powers (bottom left) in the 1 mm (green) and 4 mm (blue) detectors as a function of time. (Right) Correlated noise level vs left + right bias powers. Dashed lines show fit models, representing shot noise that scales in rate with detector volume with a shot noise quantum of $\varepsilon = 0.68 \pm 0.38$ meV, comparable to the aluminum superconducting bandgap.

superconducting bandgap energy, $2\,\Delta_{Al} \approx 360\mu$ eV, below which athermal phonons do not break Cooper pairs in the aluminum phonon collection fins of our sensors.

In addition to this phonon burst shot noise from *below* threshold events, we observe a high rate of *above*-threshold background events (often called the "Low Energy Excess," or LEE[11,12]). To investigate these LEE events, we recorded 2 or 12 h periods of continuous background data following each calibration run and triggered this dataset offline using an optimum filter optimized to search for events with a channel energy partition and pulse shape consistent with that of substrate absorbed calibration photons as in Ref. 18. In Fig. 5, bottom left, a scatterplot shows the energy deposited in each channel without a constraint on the partition. Identical to observations in Ref. 14, the LEE backgrounds split into two classes: "shared" events with an approximately equal channel partition and a pulse shape identical to substrate absorbed photons, and "single" events where nearly all energy is deposited in a single phonon sensor channel. Singles have a pulse shape with a fast rise, but a slow fall consistent with an energy deposition that saturates a subset of the athermal phonon sensors that are readout in parallel within a channel.[14] Each event is then fit with a multichannel optimum filter whose pulse shape and channel partition are fixed to the average of each LEE class (singles left, singles right, and shared) and classified according to lowest $\Delta\chi^2$.[14,18]

Similar to our observations of correlated phonon noise, we see that the rate of above-threshold shared background events scales with the detector thickness, as it does for below threshold phonon shot noise (the y-axis has been normalized by substrate mass, proportional to detector thickness). However, the rate of these high energy above-threshold shared events is consistent with being constant with time on these short timescales. At lower energies, where statistics are better, the rate of shared LEE events does appear to decrease over time.

As in Ref. 14, our singles appear to originate within the aluminum QET films, and we additionally observe that their rate decreases with time (see further discussion in supplementary material Sec. F). These observations give additional support to the proposal that dislocation mediated relaxation of thermal stress in these aluminum QET films is responsible for these singles.[14,26]

We observe that both the correlated phonon noise level and the shared LEE backgrounds scale with the detector substrate thickness. From this scaling alone, we conclusively reject the hypotheses that our aluminum or tungsten sensor films constitute the dominant source of shared phonon bursts.[26] Likewise, the phonon bursts are unlikely to originate from the top and bottom polished 1 cm^2 silicon faces of the substrate.

This thickness scaling observation is compatible with a phonon burst process whose rate scales with the diced sidewall area, the mass, or the volume of the substrate. To discriminate between these hypotheses, we would ideally measure shared LEE and correlated noise rates in detectors with different volume to sidewall ratios while keeping all other detector characteristics fixed. Unfortunately, this study with strict extraneous variable control has not been done.

However, we have characterized the LEE rate in two large area Cryogenic Photon Detectors (CPDs).[23,24] These large area cylindrical substrates (diameter: 76.2 mm, thickness 1 mm) have $\sim \times 8$ larger volume to sidewall ratio than the 1 cm^2 detectors discussed to this point. We observe good agreement with volume scaling and find that when scaling by sidewall area, both noise and above-threshold backgrounds

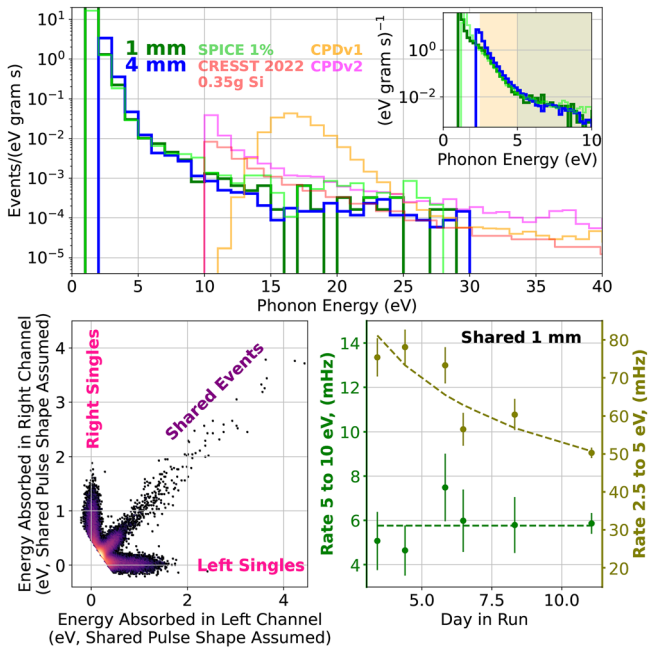

FIG. 5. (Top) The mass normalized shared background rates in the 1 and 4 mm detectors, with backgrounds measured in the SPICE 1%,[14,18] CPDv1,[23,24] CPDv2 (previously unpublished), and CRESST 0.35 g Si[25] detectors. Broadly, all six detectors seem to observe the same backgrounds normalizing for mass. Note that as the CPD and CRESST detectors are one channel detectors, which cannot reject singles,[14] the increased background rates near threshold could be due to singles as well as noise triggers or additional LEE backgrounds. For clarity, the 1 mm, 4 mm, and SPICE 1% detectors have their spectra cut off at 30 eV to remove saturated events from cosmic rays and radioactive backgrounds, which begin to appear at these energies. (Top insert) Detail of the 1 mm, 4 mm, and SPICE 1% detector backgrounds. The orange and green bands show the energy ranges in which time dependence was measured (see bottom right). (Left bottom) Background event energy partitioning between left and right channels, showing single and shared events. Note the energy reconstruction assumes a shared pulse shape in each channel. (Right bottom) Rate of shared events over time in the 1 mm detector in the shaded 2.5–5 and 5–10 eV bins in the center top figure. Dashed line shows the (weighted) average rate in the 5–10 eV range, and a power law fit in the 2.5–5 eV bin.

differ between these two sets of detectors by around an order of magnitude. While the differences in holding method, fabrication, handling, and storage history detract from our ability to control extraneous variables, we believe that the evidence for volume scaling is compelling (see the supplementary material Sec. H for additional discussion of these systematics).

Volume scaling suggests that defects in the detector substrate are responsible for LEE and excess phonon noise observations. For example, the relaxation of neutron induced crystal damage discussed in Refs. 27 and 28 could create phonon bursts consistent with our observations. The strong rate vs time since cooldown dependence we observe in our noise data, for example, could be explained by assuming that meV-scale gaps between different energy levels in defects are thermally populated at 300 K and then relax to lower energy states at mK temperatures. The observation of time dependence in above-threshold LEE rates, both here and previously,[25] is more difficult to explain, given their eV scale energies are much larger than room temperature

energy scales. As discussed in Ref. 27, an avalanche-like process where the relaxation of a meV-scale state triggers the release of many more such states is one possible mechanism by which the relaxation of thermally populated states can trigger eV scale events.

Since the shared LEE phonon bursts we observe have been shown to originate in the silicon substrate, it is likely that they would also occur in other devices constructed on silicon substrates such as superconducting qubits and MKID detectors. Phonon bursts produced in the silicon substrate would be expected to create quasiparticles in the device's superconductors, contributing to the excess equilibrium quasiparticle density long observed in these devices. To make a rough estimate of the importance of this quasiparticle generation mechanism compared to other sources, we assume that the "reduced" quasiparticle density $x_{qp} = n_{qp}/n_{cp}$ in an aluminum superconductor follows the dynamical equation:

$$\frac{dx_{qp}}{dt} = -rx_{qp}^2 + g, \tag{5}$$

where $r \approx (20\text{ns})^{-1}$ is the prefactor for the quasiparticle density dependent recombination rate and g is the normalized quasiparticle generation rate,[29–31] i.e., the rate at which phonons create quasiparticles. x_{qp} is the reduced quasiparticle density, the ratio of the quasiparticle number density n_{qp} to the Cooper pair density $n_{cp} \approx 4 \times 10^6 \mu\text{m}^{-3}$. We assume that the quasiparticle dynamics in the superconductor are dominated by recombination as in Ref. 30.

Modeling the device as a silicon substrate with an aluminum superconducting region (including qubits, KIDs, and ground planes) on the surface of the chip, we assume for simplicity that LEE events are evenly distributed through the bulk silicon chip, collected uniformly in the aluminum, and neglect any source of quasiparticle generation besides LEE phonon bursts originating in the substrate (e.g., high energy backgrounds[30] and infrared radiation[32]). This produces an average normalized quasiparticle generation rate 'of

$$\langle g \rangle = \frac{\langle \rho_p \rangle}{2\Delta_{Al} n_{cp}} \frac{V_{Si}}{V_{Al}}, \tag{6}$$

where $\langle \rho_p \rangle$ is the average LEE power density that we estimate as $\mathcal{O}[1\text{fW}/(1\,\text{cm}^2 \times 1\,\text{mm})]$ from Fig. 4 bottom left and V_{Si} and V_{Al} are the volumes of the silicon substrate and aluminum superconductor, respectively. Assuming the temporal variation in g is small compared to its average value $\langle g \rangle$, Eq. (5) can be Taylor expanded to zeroth order to find the reduced equilibrium density

$$\langle x_{qp} \rangle = \sqrt{\frac{\langle g \rangle}{r}} = \sqrt{\frac{\langle \rho_p \rangle}{2\Delta_{Al} n_{cp}} \frac{V_{Si}}{V_{Al}} \frac{1}{r}}. \tag{7}$$

For the aluminum KID on a silicon substrate described in Ref. 33, we expect a residual density of roughly $x_{qp} \approx 4 \times 10^{-6}$ created by low energy phonon bursts originating from the substrate, which compares favorably to the $x_{qp} = 4.6 \times 10^{-6}$ that they observed in their KID resonator. This technique can also be used to estimate the residual quasiparticle density caused in qubits (taking into account both the $\mathcal{O}(100\,\text{nm})$ thick qubit and ground plane, which cover nearly all the surface of the chip) and gives $x_{qp} \approx 10^{-8} - 10^{-7}$, roughly in line with observations for modern non-gap-engineered qubits.[32] Our observations also agree with the phonon origin[34] and reduction in the rate over time[34,35] previously observed for such bursts in superconducting quantum devices constructed on silicon substrates.

See the supplementary material for eight sections, which provide additional explanation of our methods. These sections discuss the following:

- Our phonon collection efficiency measurements over time
- The effects of mixture chamber cooling
- Our data quality cuts
- Uncorrelated noise, and our methods for reconstructing this noise term
- The shot noise generated from a given spectrum of small events
- The saturation and time dependence of our singles
- A comparison of the time dependence of our above-threshold event rates and excess noise sources
- Data and arguments comparing the scaling of excess shot noise and LEE backgrounds with detector volume as opposed to sidewall area

This work was supported in part by DOE Grants DE-SC0019319, DE-SC0025523, DE-SC0020374, and DE-SC0010004, and DOE Quantum Information Science Enabled Discovery (QuantISED) for High Energy Physics (KA2401032). This material is based upon work supported by the National Science Foundation Graduate Research Fellowship under Grant No. DGE 1106400. This material is based upon work supported by the Department of Energy National Nuclear Security Administration through the Nuclear Science and Security Consortium under Award Nos. DE-NA0003180 and/or DE-NA0000979. Work at Lawrence Berkeley National Laboratory was supported by the U.S. DOE, Office of High Energy Physics, under Contract No. DEAC02-05CH11231. Work at Argonne is supported by the U.S. DOE, Office of High Energy Physics, under Contract No. DE-AC02-06CH11357. W.G. and Y.Q. acknowledge the support by the National High Magnetic Field Laboratory at Florida State University, which is supported by the National Science Foundation Cooperative Agreement No. DMR-2128556 and the State of Florida.

AUTHOR DECLARATIONS

Conflict of Interest

The authors have no conflicts to disclose.

Author Contributions

C. L. Chang: Funding acquisition (equal); Project administration (equal); Validation (equal); Writing – review & editing (equal). **Y.-Y. Chang:** Investigation (equal); Methodology (equal); Resources (equal); Writing – review & editing (equal). **M. Garcia-Sciveres:** Funding acquisition (equal); Project administration (equal); Resources (equal); Writing – review & editing (equal). **W. Guo:** Funding acquisition (equal); Project administration (equal); Resources (equal); Writing – review & editing (equal). **S. A. Hertel:** Funding acquisition (equal); Investigation (equal); Methodology (equal); Supervision (equal); Validation (equal); Writing – review & editing (equal). **X. Li:** Methodology (equal); Software (equal); Writing – review & editing

(equal). **J. Lin:** Funding acquisition (equal); Project administration (equal); Writing – review & editing (equal). **M. Lisovenko:** Writing – review & editing (equal). **R. Mahapatra:** Funding acquisition (equal); Investigation (equal); Methodology (equal); Resources (equal); Writing – review & editing (equal). **W. Matava:** Data curation (equal); Software (equal); Writing – review & editing (equal). **D. N. McKinsey:** Funding acquisition (lead); Investigation (equal); Methodology (equal); Project administration (equal); Resources (equal); Supervision (equal); Writing – review & editing (equal). **P. K. Patel:** Software (equal); Writing – review & editing (equal). **B. Penning:** Funding acquisition (equal); Project administration (equal); Resources (equal); Writing – review & editing (equal). **H. D. Pinckney:** Data curation (equal); Formal analysis (equal); Methodology (equal); Writing – review & editing (equal). **M. Platt:** Methodology (equal); Resources (lead); Writing – review & editing (equal). **M. Pyle:** Conceptualization (equal); Formal analysis (equal); Funding acquisition (equal); Investigation (equal); Methodology (equal); Project administration (equal); Resources (equal); Software (equal); Supervision (equal); Validation (equal); Writing – original draft (equal); Writing – review & editing (equal). **Y. Qi:** Writing – review & editing (equal). **M. Reed:** Data curation (equal); Formal analysis (equal); Investigation (equal); Methodology (equal); Resources (equal); Software (equal); Validation (equal); Writing – review & editing (equal). **I. Rydstrom:** Data curation (equal); Methodology (equal); Resources (equal); Software (equal); Writing – review & editing (equal). **R. K. Romani:** Conceptualization (equal); Data curation (lead); Formal analysis (lead); Methodology (equal); Resources (equal); Software (equal); Validation (equal); Visualization (lead); Writing – original draft (lead); Writing – review & editing (equal). **B. Sadoulet:** Funding acquisition (equal); Project administration (equal); Resources (equal); Supervision (equal); Writing – review & editing (equal). **B. Serfass:** Data curation (equal); Formal analysis (equal); Investigation (equal); Methodology (equal); Project administration (equal); Resources (equal); Software (lead); Supervision (equal); Writing – review & editing (equal). **P. Sorensen:** Conceptualization (equal); Data curation (equal); Formal analysis (equal); Investigation (equal); Supervision (equal); Writing – review & editing (equal). **B. Suerfu:** Resources (equal); Writing – review & editing (equal). **V. Velan:** Methodology (equal); Resources (equal); Software (equal); Writing – review & editing (equal). **G. Wang:** Project administration (equal); Resources (equal); Writing – review & editing (equal). **Y. Wang:** Writing – review & editing (equal). **M. R. Williams:** Conceptualization (equal); Methodology (equal); Resources (equal); Software (equal); Validation (equal); Writing – review & editing (equal). **V. G. Yefremenko:** Methodology (equal); Resources (equal); Writing – review & editing (equal).

DATA AVAILABILITY

The data that support the findings of this study are available from the corresponding author upon reasonable request.

REFERENCES

[1]E. Kuflik, M. Perelstein, N. R.-L. Lorier, and Y.-D. Tsai, "Elastically decoupling dark matter," Phys. Rev. Lett. **116**, 221302 (2016).

[2]E. Kuflik, M. Perelstein, N. R.-L. Lorier, and Y.-D. Tsai, "Phenomenology of ELDER dark matter," J. High Energy Phys. **2017**, 78.

[3]Y. Hochberg, E. Kuflik, T. Volansky, and J. G. Wacker, "Mechanism for thermal relic dark matter of strongly interacting massive particles," Phys. Rev. Lett. **113**, 171301 (2014).

[4]Y. Hochberg, E. Kuflik, H. Murayama, T. Volansky, and J. G. Wacker, "Model for thermal relic dark matter of strongly interacting massive particles," Phys. Rev. Lett. **115**, 021301 (2015).

[5]L. J. Hall, K. Jedamzik, J. March-Russell, and S. M. West, "Freeze-in production of FIMP dark matter," J. High Energy Phys. **2010**, 80.

[6]J. Billard, R. Carr, J. Dawson *et al.*, "Coherent neutrino scattering with low temperature bolometers at Chooz reactor complex," J. Phys. G **44**, 105101 (2017).

[7]C. Goupy, H. Abele, G. Angloher, A. Bento, L. Canonica, F. Cappella, L. Cardani, N. Casali, R. Cerulli, I. Colantoni, A. Cruciani, G. Del Castello, M. d G. Roccagiovine, A. Doblhammer, S. Dorer, A. Erhart, M. Friendl, A. Garai, V. M. Ghete, D. Hauff, F. Jeanneau, E. Jericha, M. Kaznacheeva, A. Kinast, H. Kluck, A. Langenkämper, T. Lasserre, D. Lhuillier, M. Mancuso, B. Mauri, A. Mazzolari, E. Mazzucato, H. Neyrial, C. Nones, L. Oberauer, T. Ortmann, L. Pattavina, L. Peters, F. Petricca, W. Potzel, F. Pröbst, F. Pucci, F. Riendl, R. Rogly, M. Romagnoni, J. Rothe, N. Schermer, J. Schieck, S. Schönert, C. Schwertner, L. Scola, G. S. Sidikov, L. Stodolsky, R. Strauss, M. Tamisari, C. Tomei, M. Vignati, M. Vivier, V. Wagner, A. Wex, and NUCLEUS Collaboration, "Exploring coherent elastic neutrino-nucleus scattering of reactor neutrinos with the nucleus experiment," SciPost. Phys. **12**, 53 (2022).

[8]R. K. Romani, Y.-Y. Chang, R. Mahapatra, M. Platt, M. Reed, I. Rydstrom, B. Sadoulet, B. Serfass, and M. Pyle, "A transition edge sensor operated in coincidence with a high sensitivity athermal phonon sensor for photon coupled rare event searches," Appl. Phys. Lett. **125**, 232601 (2024).

[9]J. Liu, K. Dona, G. Hoshino, S. Knirck, N. Kurinsky, M. Malaker, D. W. Miller, A. Sonnenschein, M. H. Awida, P. S. Barry, K. K. Berggren, D. Bowring, G. Carosi, C. Chang, A. Chou, R. Khatiwada, S. Lewis, J. Li, S. W. Nam, O. Noroozian, and T. X. Zhou, "Broadband solenoidal haloscope for terahertz axion detection," Phys. Rev. Lett. **128**, 131801 (2022).

[10]J. Chiles, I. Charaev, R. Lasenby, M. Baryakhtar, J. Huang, A. Roshko, G. Burton, M. Colangelo, K. Van Tilburg, A. Arvanitaki, S. W. Nam, and K. K. Berggren, "New constraints on dark photon dark matter with superconducting nanowire detectors in an optical haloscope," Phys. Rev. Lett. **128**, 231802 (2022).

[11]P. Adari, A. A. Aguilar-Arevalo, D. Amidei *et al.*, "EXCESS workshop: Descriptions of rising low-energy spectra," SciPost Phys. Proc. **9**, 1 (2022).

[12]D. Baxter, R. Essig, Y. Hochberg, M. Kaznacheeva, B. von Krosigk, F. Reindl, R. K. Romani, and F. Wagner, "Low-energy backgrounds in solid-state phonon and charge detectors," arXiv:2503.08859 (2025).

[13]G. Angloher, S. Banik, G. Benato, A. Bento, A. Bertolini, R. Breier, C. Bucci, J. Burkhart, L. Canonica, A. D'Addabbo, S. Di Lorenzo, L. Einfalt, A. Erb, F. v. Feilitzsch, S. Fichtinger, D. Fuchs, A. Garai, V. M. Ghete, P. Gorla, P. V. Guillaumon, S. Gupta, D. Hauff, M. Ješkovský, J. Jochum, M. Kaznacheeva, A. Kinast, H. Kluck, H. Kraus, S. Kuckuk, A. Langenkämper, M. Mancuso, L. Marini, B. Mauri, L. Meyer, V. Mokina, M. Olmi, T. Ortmann, C. Pagliarone, L. Pattavina, F. Petricca, W. Potzel, P. Povinec, F. Pröbst, F. Pucci, F. Reindl, J. Rothe, K. Schäffner, J. Schieck, S. Schönert, C. Schwertner, M. Stahlberg, L. Stodolsky, C. Strandhagen, R. Strauss, I. Usherov, F. Wagner, V. Wagner, and V. Zema, "DoubleTES detectors to investigate the CRESST low energy background: Results from above-ground prototypes," Eur. Phys. J. C **84**, 1001 (2024).

[14]R. Anthony-Petersen, C. L. Chang, Y.-Y. Chang, L. Chaplinsky, C. W. Fink, M. Garcia-Sciveres, W. Guo, S. A. Hertel, X. Li, J. Lin, M. Lisovenko, R. Mahapatra, W. Matava, D. N. McKinsey, D. Z. Osterman, P. K. Patel, B. Penning, M. Platt, M. Pyle, Y. Qi, M. Reed, I. Rydstrom, R. K. Romani, B. Sadoulet, B. Serfass, P. Sorensen, B. Suerfu, V. Velan, G. Wang, Y. Wang, S. L. Watkins, and M. R. Williams, "Low energy backgrounds and excess noise in a two-channel low-threshold calorimeter," Appl. Phys. Lett. **126**, 102601 (2025).

[15]K. D. Irwin, S. W. Nam, B. Cabrera, B. Chugg, and B. A. Young, "A quasiparticle-trap-assisted transition-edge sensor for phonon-mediated particle detection," Rev. Sci. Instrum. **66**, 5322–5326 (1995).

[16]R. K. Romani, "Correlated and uncorrelated backgrounds and noise sources in athermal phonon detectors and other low temperature devices," in 20th International Conference on Low Temparature Detectors (2023).

[17]R. Anthony-Petersen, A. Biekert, R. Bunker *et al.*, "A stress-induced source of phonon bursts and quasiparticle poisoning," Nat. Commun. **15**, 6444 (2024).

[18]C. L. Chang, Y. Y. Chang, L. Chaplinsky, C. W. Fink, M. Garcia-Sciveres, W. Guo, S. A. Hertel, X. Li, J. Lin, M. Lisovenko, R. Mahapatra, W. Matava, D. N. McKinsey, V. Novati, P. K. Patel, B. Penning, H. D. Pinckney, M. Platt, M. Pyle,

Y. Qi, M. Reed, G. R. C. Rischbieter, R. K. Romani, B. Sadoulet, B. Serfass, P. Sorensen, A. Suzuki, V. Velan, G. Wang, Y. Wang, S. L. Watkins, M. R. Williams, J. K. Wuko, T. Aramaki, P. Cushman, N. N. Gite, A. Gupta, M. E. Huber, N. A. Kurinsky, J. S. Mammo, B. von Krosigk, A. J. Mayer, J. Nelson, S. M. Oser, L. Pandey, A. Pradeep, W. Rau, and T. Saab, "First limits on light dark matter interactions in a low threshold two channel athermal phonon detector from the TESSERACT collaboration," Phys. Rev. Lett. **135**, 161002 (2025).

[19]E. Michielin, "HVeV detectors down at Cute," in eXCESS 2024 Workshop (2024).

[20]G. Angloher, S. Banik, G. Benato, A. Bento, A. Bertolini, R. Breier, C. Bucci, J. Burkhart, L. Canonica, A. D'Addabbo, S. Di Lorenzo, L. Einfalt, A. Erb, F. Feilitzsch, S. Fichtinger, D. Fuchs, A. Garai, V. Ghete, P. Gorla, P. Guillaumon, S. Gupta, D. Hauff, M. Ješkovský, J. Jochum, M. Kaznacheeva, A. Kinast, H. Kluck, H. Kraus, S. Kuckuk, A. Langenkämper, M. Mancuso, L. Marini, B. Mauri, L. Meyer, V. Mokina, M. Olmi, T. Ortmann, C. Pagliarone, L. Pattavina, F. Petricca, W. Potzel, P. Povinec, F. Pröbst, F. Pucci, F. Reindl, J. Rothe, K. Schäffner, J. Schieck, S. Schönert, C. Schwertner, M. Stahlberg, L. Stodolsky, C. Strandhagen, R. Strauss, I. Usherov, F. Wagner, V. Wagner, and V. Zema, "First observation of single photons in a CRESST detector and new dark matter exclusion limits," Phys. Rev. D **110**, 083038 (2024).

[21]M. A. Lindeman, B. Dirks, J. van der Kuur, P. A. J. de Korte, R. H. den Hartog, L. Gottardi, R. A. Hijmering, H. F. C. Hoevers, and P. Khosropanah, "Relationships between complex impedance, thermal response, and noise in TES calorimeters and bolometers," IEEE Trans. Appl. Supercond. **21**, 254–257 (2011).

[22]K. Irwin and G. Hilton, "Transition-Edge sensors," in *Cryogenic Particle Detection, Topics in Applied Physics*, edited by C. Enss (Springer, Berlin, Heidelberg, 2005), pp. 63–150.

[23]C. W. Fink, S. L. Watkins, T. Aramaki, P. L. Brink, J. Camilleri, X. Defay, S. Ganjam, Y. G. Kolomensky, R. Mahapatra, N. Mirabolfathi, W. A. Page, R. Partridge, M. Platt, M. Pyle, B. Sadoulet, B. Serfass, S. Zuber, and CPD Collaboration, "Performance of a large area photon detector for rare event search applications," Appl. Phys. Lett. **118**, 022601 (2021).

[24]I. Alkhatib, D. Amaral, T. Aralis *et al.*, SuperCDMS Collaboration, "Light dark matter search with a high-resolution athermal phonon detector operated above ground," Phys. Rev. Lett. **127**, 061801 (2021).

[25]G. Angloher, S. Banik, G. Benato *et al.*, "Latest observations on the low energy excess in CRESST-III," SciPost Phys. Proc. **12**, 13 (2023).

[26]R. K. Romani, "Aluminum relaxation as the source of excess low energy events in low threshold calorimeters," J. Appl. Phys. **136**, 124502 (2024).

[27]K. Nordlund, F. Kong, F. Djurabekova, M. Heikinheimo, K. Tuominen, and N. Mirabolfathi, "Spontaneous damage annealing reactions as a possible source of low energy excess in semiconductor detectors," Phys. Rev. Materials **9**, 113603 (2025).

[28]A. Jay, M. Raine, N. Richard, N. Mousseau, V. Goiffon, A. Hemeryck, and P. Magnan, "Simulation of single particle displacement damage in silicon–Part II: Generation and long-time relaxation of damage structure," IEEE Trans. Nucl. Sci. **64**, 141–148 (2017).

[29]J. Martinis, "Saving superconducting quantum processors from decay and correlated errors generated by gamma and cosmic rays," npj Quantum Inf. **7**, 90 (2021).

[30]A. P. Vepsäläinen, A. H. Karamlou, J. L. Orrell, A. S. Dogra, B. Loer, F. Vasconcelos, D. K. Kim, A. J. Melville, B. M. Niedzielski, J. L. Yoder, S. Gustavsson, J. A. Formaggio, B. A. VanDevender, and W. D. Oliver, "Impact of ionizing radiation on superconducting qubit coherence," Nature **584**, 551–556 (2020).

[31]C. Wang, Y. Y. Gao, I. M. Pop, U. Vool, C. Axline, T. Brecht, R. W. Heeres, L. Frunzio, M. H. Devoret, G. Catelani, L. I. Glazman, and R. J. Schoelkopf, "Measurement and control of quasiparticle dynamics in a superconducting qubit," Nat. Commun. **5**, 5836 (2014).

[32]K. Serniak, M. Hays, G. de Lange, S. Diamond, S. Shankar, L. Burkhart, L. Frunzio, M. Houzet, and M. Devoret, "Hot nonequilibrium quasiparticles in transmon qubits," Phys. Rev. Lett. **121**, 157701 (2018).

[33]D. J. Temples, O. Wen, K. Ramanathan, T. Aralis, Y.-Y. Chang, S. Golwala, L. Hsu, C. Bathurst, D. Baxter, D. Bowring, R. Chen, E. Figueroa-Feliciano, M. Hollister, C. James, K. Kennard, N. Kurinsky, S. Lewis, P. Lukens, V. Novati, R. Ren, and B. Schmidt, "Performance of a phonon-mediated kinetic inductance detector at the nexus cryogenic facility," Phys. Rev. Appl. **22**, 044045 (2024).

[34]E. Yelton, C. P. Larson, K. Dodge, K. Okubo, and B. L. T. Plourde, "Correlated quasiparticle poisoning from phonon-only events in superconducting qubits," Phys. Rev. Lett. **135**(12), 123601 (2025).

[35]E. T. Mannila, P. Samuelsson, S. Simbierowicz, J. T. Peltonen, V. Vesterinen, L. Gronberg, J. Hassel, V. F. Maisi, and J. P. Pekola, "A superconductor free of quasiparticles for seconds," Nat. Phys. **18**, 145–148 (2022).